J Sol-Gel Sci Technol (2007) 44:269–273
DOI 10.1007/s10971-007-1629-4

ORIGINAL PAPER

Ferroelectric and dielectric behaviour of $Bi_{0.92}La_{0.08}FeO_3$ multiferroic thin films prepared by soft chemistry route

Alexandre Z. Simões · Laecio Santos Cavalcante · Carla Santos Riccardi · José A. Varela · Elson Longo

Received: 2 July 2007 / Accepted: 11 September 2007 / Published online: 3 October 2007

Abstract $Bi_{0.92}La_{0.08}FeO_3$ (BLFO) thin films were grown on platine substrates by the soft chemical route. Ferroelectric and dielectric behaviors of BLFO films deposited by spin-coating technique and annealed at 773 K for 2 h in air atmosphere were explained. BLFO thin films obtained presents a rhombohedral structure. The BLFO films present dielectric and ferroelectric behaviors with dielectric permittivity and dielectric loss of approximately 81 and 0.0144 at 1 kHz. The Au/BLFO/Pt capacitor shows a hysteresis loop with remnant polarization of 20.6 $\mu C/cm^2$ and coercive field of 53.88 kV/cm. The polarization switching and the fatigue behavior of the BLFO films were significantly enhanced.

A. Z. Simões
Faculdade de Ciêencias, Departamento de Química, Universidade Estadual Paulista, Av. Luiz Edmundo Carrijo Coube, 14-01, Vargem Limpa, Bauru, SP 17033-360, Brazil
e-mail: alezipo@yahoo.com

L. S. Cavalcante (✉)
Laboratório Interdisciplinar de Eletroquímica e Cerâmica, Departamento de Química, Universidade Federal de São Carlos, P.O. Box 676, Sao Carlos, SP 13565-905, Brazil
e-mail: laeciosc@bol.com.br

C. S. Riccardi · J. A. Varela · E. Longo
Laboratório Interdisciplinar em Cerâmica, Departamento de Físico-Química, Instituto de Química, Universidade Estadual Paulista, P.O. Box 355, Araraquara, SP 14801-907, Brazil

C. S. Riccardi
e-mail: cariccardi@yahoo.com

J. A. Varela
e-mail: varela@iq.unesp.br

E. Longo
e-mail: elson@iq.unesp.br

Keywords Ferroelectrics · Dielectric · Microstructure · $BiFeO_3$ · Thin films

1 Introduction

Perovskites such as $BiFeO_3$ (BFO) [1], $BiMnO_3$ [2], $TbMnO_3$ [3], and $TbMn_2O_5$ [4] have recently attracted very attention, due the potential to provide a wide range of applications, including the emerging field of spintronics [5], data-storage media [6] and multiple-state memories [7]. The BFO is known to be the only material that exhibits ferromagnetism at room temperature [8]. It is a rhombohedrally distorted ferroelectric perovskite (T_C = 1,043 K) with the space group $R3_c$ [9] and shows *G*-type antiferromagnetism up to 643K (T_N) [10]. The specific characteristics, such as a simple crystal structure, a high Curie temperature (electrical), and a high Néel temperature (magnetic), are advantageous for research and various applications [11].

In bismuth-based ferroelectrics, such as $Bi_4Ti_3O_{12}$ [12] and $SrBi_4Ti_4O_{15}$ [13], the doping of lanthanum (La) was effective to enhance the insulating and ferroelectric properties because of the reduced oxygen vacancy stabilizes the oxygen octahedron [14]. Some studies reported in literature [15, 16, 17] suggest that the inhomogeneous magnetic spin structure can be effectively suppressed by La doping. Therefore, the influence of La doping on polarization switching, ferroelectric reliability, and multiferroic properties of BFO films require more attention [18].

BFO pure or doped films have been fabricated by several methods such as physics: pulsed laser deposition (PLD) [19], rf-magnetron sputtering [20], molecular bean epitaxy (MBE) [21] and chemistry: Sol–gel [22], Metalorganic

chemical vapor deposition (MCVD) [23], chemical solution deposition [24]. All present advantages and disadvantages. However, chemical methods have advantages in relation to physics method due their precise control of chemical composition, homogeneity, microstructure and dielectric characteristics [25].

In this way, we reported the preparation of $Bi_{0.92}La_{0.08}FeO_3$ (BLFO) thin films grown on Pt(111)/Ti/SiO_2/Si substrates with good structural, microstructural and electrical properties at room temperature by the polymeric precursor method.

2 Experimental details

2.1 Synthesis of $Bi_{0.92}La_{0.08}FeO_3$ thin films

Iron (III) nitrate nonahydrate, 99.5% purity (Merck), bismuth nitrate, 99.5% purity (Aldrich) and lanthanum acetate, 99.9% purity (Aldrich) were used as raw materials. The precursor solutions of bismuth and iron were prepared by adding the raw materials to ethylene glycol and concentrated aqueous citric acid under heating and stirring at 333 K. Appropriate quantities of solutions of Fe and Bi were mixed and homogenized by stirring at 363 K. The loss of bismuth oxide is monitored by measuring the weight change of the powder before and after heat treatment of the material in powder dispersed. Thus, an excess of 5 wt% Bi was added to the solution, aiming to minimize the bismuth loss during annealing. This Bi excess is employed for compensate the volatilization of bismuth. Without bismuth addition, single phase BFLO thin film could not be obtained. The temperature increases and no use of Bi excess, favors the presence of deleterious phase, such as $Bi_2Fe_4O_9$, $Bi_{1.88}La_{0.12}O_3$ and $Bi_{36}La_{0.08}Fe_{42}O_{57}$, more details in Ref. [24]. The molar ratio of metal/citric acid/ethylene glycol was 1/4/16. The viscosity of the resulting solution was adjusted to 20 cP by controlling the water content using a Brookfield viscosimeter. The BLFO thin films were spin coated on Pt(111)/Ti/SiO_2/Si substrates by a commercial spinner operating at 5,000 rpm for 10 s (spin-coater KW-4B, Chemat Technology). After deposition, the BLFO films were kept at 423 K on a hot plate for 10 min to remove residual solvents. The heat treatment was carried out in two stages: initial heating at 573 K for 2 h at a heating rate of 274 K/min to promote the pyrolysis of the organic materials, and finally the films were annealed at 773 K for 2 h at a heating rate of 274 K/min. The four CZT layers were obtained crystallizing each layer in a furnace for 2 h under air atmosphere until the desired thickness was reached.

2.2 Characterizations of $Bi_{0.92}La_{0.08}FeO_3$ thin films

In these experiments, BLFO thin films were characterized by X-ray diffraction (XRD) patterns recorded on a (Rigaku-DMax 2500PC, Japan) with Cu-Kα radiation in the 2θ range from 20 to 60° with 0.02°/min. The microstructure of the thin films was examined using atomic force microscopy (AFM) (Digital Instruments, Nanoscope IIIa) and thickness was evaluated by observing the cross-section of the films using a high-resolution field-emission gun scanning electron microscopy FEG-SEM (Supra 35-VP, Carl Zeiss). The Au top electrode area 3×10^{-4} cm^2 was deposited by sputtering through a designed mask onto the film surfaces. The relative dielectric constant (ε_r) was measured versus frequency using an impedance analysis (model 4192 A, Hewlett Packard). The capacitance–voltage characteristic was measured in the Au/BLFO/Pt configuration using a small AC signal of 10 mV at 100 kHz. The AC signal was applied across the sample, while the DC was swept from positive to negative bias. Ferroelectricity was investigated using a Sawyer-Tower circuit attached to a computer controlled standardized ferroelectric test system (Radiant Technology 6000 A). For the fatigue measurements, internally generated 8.6 μs wide square pulses or externally generated square pulses was used. After the end of each fatigue period, the polarization characteristic of the films was measured over a range of frequencies.

3 Results and discussion

3.1 X-ray diffraction analysis

Figure 1 displayed the XRD pattern of BLFO thin films annealed at 773 K for 2 h.

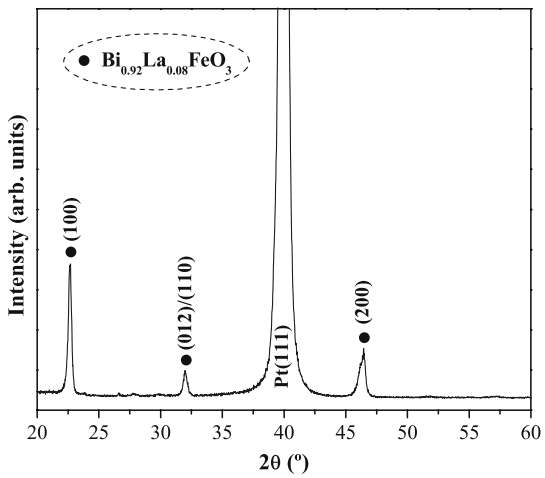

Fig. 1 XRD patterns of BLFO film annealed at 773 K for 2 h in air atmosphere

As can be seen, a single perovskite phase free of impurities was obtained. The diffraction peaks were identified using the rhombohedral structure. The intensity of (100) and (200) diffraction peaks were stronger with respect to that of the (110) and (012) peak. The (100) and (200) out-of-plane preferred orientation due to the self-textured.

The orientation of the film was changed to (100) and (200) preferred orientation due to the self-textured.

3.2 Atomic force microscopy analysis

Figure 2 shows the surface morphology of BLFO thin films deposited on Pt substrates.

$Bi_{0.92}La_{0.08}FeO_3$ (BLFO) thin films exhibited bimodal distributed grains low porosity and roughness low. The medium diameter of the grains and medium surface roughness were calculated by means from Nanoscope IIIa software-2003 (Version 5.12r5 for Windows XP professional). The root mean square surface roughness of BLFO films were 4 nm. The grain sizes were estimated to be approximately in range of 58 for 62 nm. The larger number of nucleation sites provided by Pt substrates was probably responsible for some small grain size of the BLFO films. Singh et al. [22] showed that the surface morphology of the films varied with an increase in La-substitution concentration. In a 5% La-substituted film, the size of the merged boulders decreased to 0.5–1 μm diameter with island-like morphology. In a 10% La-substituted BFO film, these rounded grains became transformed into elongated grains with 0.2 μm wide and 0.2–0.4 μm long. In our films a great improvement in average reported that the grain sizes for BLFO thin films prepared by rf-magnetron sputtering were estimated to be approximately 90 nm and a great improvement in surface roughness of the BFO films with La doping was observed. Our results presented are in agreement with literature [18, 22]. The thickness of BLFO thin film is approximately 360 nm.

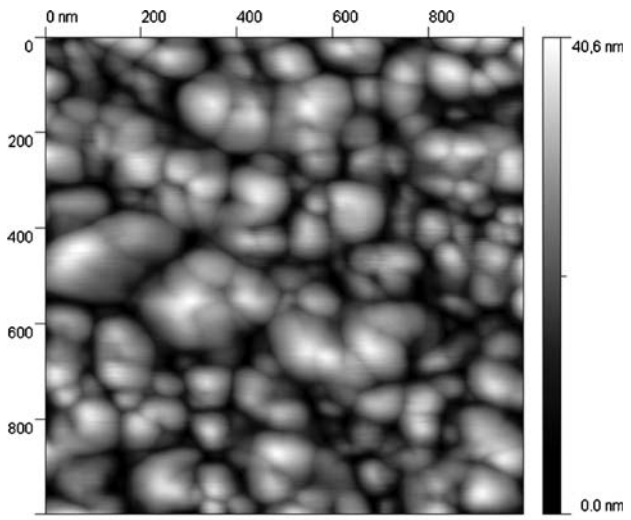

Fig. 2 AFM micrograph for BLFO thin film annealed at 773 K for 2 h in air atmosphere

3.3 Dielectric and ferroelectric properties analysis

Figure 3 shows the frequency dependence of the dielectric constant and dielectric loss of the BLFO thin film on $Pt(111)/Ti/SiO_2/Si$ substrates.

The dielectric constant (ε_r) and dielectric loss (tan δ) value at frequency of 1 kHz were 81 and 0.0144, respectively, at room temperature. The dielectric permittivity values of BLFO thin film thermal treated at 773 K were superior to published by Gao et al. [19], that described BLFO thin film obtained by pulsed laser deposition and treated in the same temperature. In agreement with the Ref. [26], La doping enhances significantly the value of ε_r of BFO thin films as much as about three times, however a little influence on loss tan δ. Second Das et al. [27] the increase of ε_r may be attributed to the reduction of impurity in the BFO thin films. We suggest that the La addition promotes appropriate lattice distortion (or strain) in our thin films. The tan δ in all films found to increase slightly from 0.03 to 0.07 with La substitution [27]. However, in our thin films the tan δ is low compared with $Bi_{0.95}La_{0.05}FeO_3$ with tan δ of 0.23.

$Bi_{0.92}La_{0.08}FeO_3$ (BLFO) thin films deposited on $Pt(111)/Ti/SiO_2/Si$ substrates exhibit ferroelectric characteristics, as can be seen in Fig. 4.

Hysteresis loops measured at room temperature for BLFO thin films annealed at 773 K, with applied voltage of 9 V is shown. BLFO thin films presents remnant polarization (P_r) of 20.3 $\mu C/cm^2$ and coercive field (E_c) of

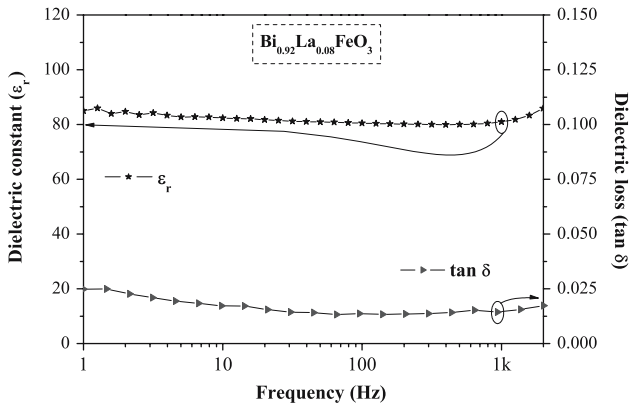

Fig. 3 Frequency dependence of the dielectric constant and dielectric loss of the BLFO thin film with a Au/BLFO/Pt configuration

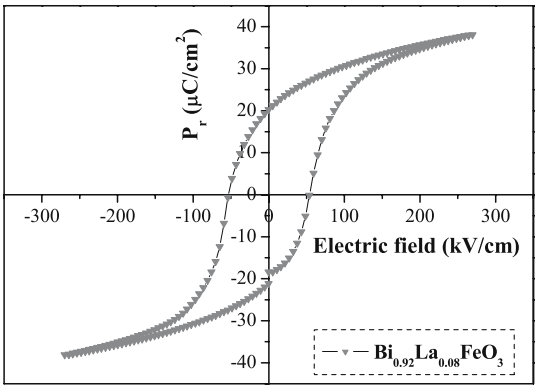

Fig. 4 P–E hysteresis loops for BLFO thin films annealed at 773 K for 2 h in air atmosphere

53.88 kV/cm. The high P_r value observed in BLFO thin films are similar with the values reported by Das et al. [27] in $Bi_{0.80}La_{0.20}FeO_3$ films and superior to reported in Ref. [28] in $Bi_{0.95}La_{0.05}FeO_3$ ceramics.

Figure 5 displays the typical capacitance–voltage (C–V) curves for BLFO thin films with the applied volt age region from 8 to –8 V.

The C–V exhibited a hysteresis loop that depended on the sweep direction of the bias voltage, confirming the dielectric properties for BLFO thin films. A general bell-shape of C–V measurement was obtained with a cycling of the bias voltage up and down at room temperature. The capacitance–voltage dependence is strongly nonlinear, confirming the dielectric properties of the film resulting from domain switching. The C–V curve is symmetric around the zero bias axis, indicating that the films contain only few movable ions or charge accumulation at the film electrode interface [29].

A typical leakage current characteristic of BLFO thin films, measured with a voltage step of 0.1 V and elapsed

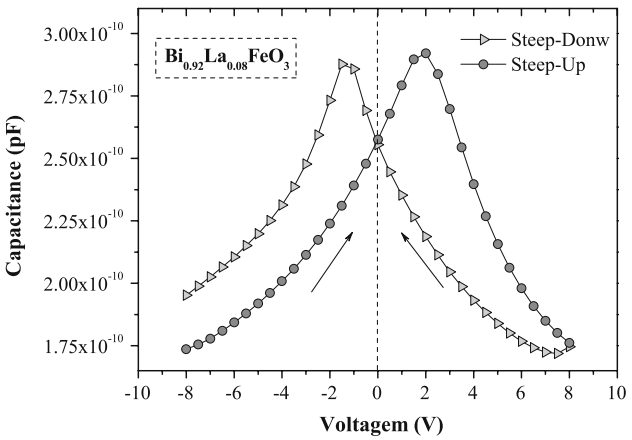

Fig. 5 Capacitance in dependence of voltage for BLFO film annealed at 773 K for 2 h in air atmosphere

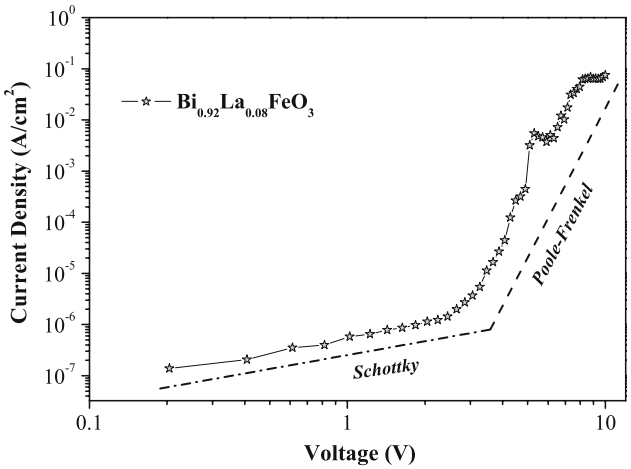

Fig. 6 Leakage current density as a function of applied voltage for BLFO thin film annealed at 773 K for 4 h in air atmosphere

time of 1.0 s for each voltage, is shown in Fig. 6. The top electrode was biased positively.

Figure 6 shows the measured current density (J) versus the electric field (E) in a log (J) versus log (E) plot for BLFO thin films. Two clearly different regions were observed. The current density increases linearly with external electric field in the low electric field region suggesting an ohmic conduction, characteristic of the Schottky emission mechanism. With increasing external field, the current density increases exponentially, characteristics of the Poole-Frenkel emission mechanism. The leakage current density levels at 3 V were 3.7×10^{-6} A/cm^2. Both the Schottky and Poole-Frenkel emissions stem from lowering a Coulombic potential barrier. Schottky emission is also considered an electrode-limited conduction mechanism and occurs at low voltages, where the electrons at the surface of a metal or semiconductor transit above the potential barrier. The Poole-Frenkel emission mechanism involves a superimposed constant electric field and a localized potential, where the applied field enhanced electron emission from Coulombic donor-like centers or holes from acceptor centers [30]. Second Pabst et al. [31], the leakage mechanisms in thin films BFO-based no clear dominant mechanism when Pt is used as the top electrode. Careful studies and attention must be given to choose a contact with the appropriate material properties to alleviate this effect.

The fatigue endurance for BLFO thin films annealed at 773 K for 2 h in air atmosphere was evaluated (Fig. 7.)

The switched polarization between two opposite polarity pulses, P^*–$P^\wedge$ or $-P^*$–$(-P^\wedge)$ denote the switchable polarization, which is an important variable for nonvolatile memory applications. Fatigue resistance was observed up to 10^7 cycles with an applied pulse voltage of 9 V for BLFO thin films in air atmosphere suggesting a good

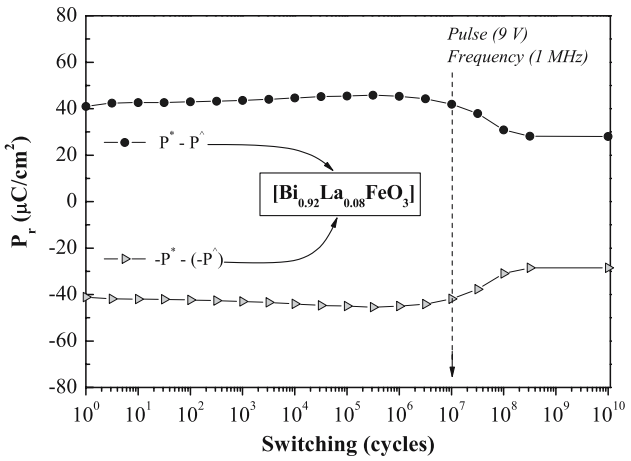

Fig. 7 Fatigue as a function of polarization cycles for BLFO thin film annealed at 773 K for 4 h in air atmosphere

potential for applications in ferroelectric memories. After 10^7 cycles the film presents fatigue characteristics that due to increase of local current around the nucleation sites which can destroy the film-electrode interface and suppress the nucleation of oppositely oriented domains at the surface. In this film an increase in switching polarization leads to a local increase in conductivity at the film-electrode interface region [32].

4 Conclusions

$Bi_{0.92}La_{0.08}FeO_3$ (BLFO) thin films were prepared by the soft chemical route. The BLFO films showed preferential polycrystalline orientations with the La-substitution in 8% in BFO films and did not show any structural distortion. The BLFO thin films consisted of bimodal grains of 58–62 nm wide, a low surface roughness (rms 4 nm) with a film thickness of 360 nm. The dielectric constant and dielectric loss at 1 kHz were 81 and 0.00144, respectively. C–V characteristic of BLFO thin films deposited at 773 K exhibited a symmetry curve in the maximum dielectric constant that was observed in the vicinity of the spontaneous polarization switch. The leakage current density at 3 V was about 3.7×10^{-6} A/cm^2. Fatigue resistance was observed with the lanthanum addition in BFO lattice. The film shows ferroelectricity behavior at room temperature.

Acknowledgements The authors thank for the financial support of the Brazilian research financing institutions: CAPES, FAPESP and CNPq.

References

1. Gonzalez AHM, Simões AZ, Cavalcante LS, Longo E, Varela JA, Riccardi CS (2007) Appl Phys Lett 90:052906
2. dos Santos AM, Parashar S, Raju AR, Zhao YS, Cheetham AK, Rao CNR (2002) Solid State Commun 122:49
3. Kimura T, Goto T, Shintani H, Ishizaka K, Arima T, Tokura Y (2003) Nature (London) 426:55
4. Hur N, Park S, Sharma PA, Ahn JS, Guha S, Cheong SW (2004) Nature (London) 429:392
5. Béa H, Bibes M, Sirena M, Herranz G, Bouzehouane K, Jacquet E, Fusil S, Paruch P, Dawber M, Contour J-P, Barthélémy A (2006) Appl Phys Lett 90:062502
6. Fiebig M, Lottermoser Th, Fröhlich D, Golsev AV, Pisarev RV (2002) Nature (London) 419:819
7. Hill NA (2000) J Phys Chem B 104:104
8. Naganuma H, Okamura S (2007) J Appl Phys 101:09M103
9. Kubel F, Schmid H (1990) Acta Crystallogr Sect B Struct Sci 46:698
10. Fischer P, Polomska M, Sosnowska I, Szymanski M (1980) J Phys C Solid State Phys 13:1931
11. Wang J, Neaton JB, Zheng H, Nagarajan V, Ogale SB, Liu B, Viehland D, Vaithyanathan V, Schlom DG, Waghmare UV, Spaldin NA, Rabe KM, Wuttig M, Ramesh R (2003) Science 229:1719
12. Simões AZ, Riccardi CS, Cavalcante LS, Longo E, Varela JA, Mizaikoff B, Hess D (2007) J Appl Phys 101:084112
13. Chen YP, Yao YY, Bao ZH, Zhu JS, Wang YN (2003) Mater Lett 57:3623
14. Kan Y, Jin X, Zhang G, Wang P, Cheng Y-B, Yan D (2004) J Mater Chem 14:3566
15. Lee D, Kim MG, Ryu S, Jang HM, Lee SG (2005) Appl Phys Lett 86:222903
16. Ederer C, Spaldin NA (2005) Phys Rev B 71:224103
17. Zhong Y, Hu G, Tang TA (2003) Jpn J Appl Phys Part 1 42:7424
18. Lee Y-H, Wu J-M, Lai C-H (2006) Appl Phys Lett 88:042903
19. Gao F, Qiu XY, Yuan Y, Xu B, Wen YY, Yuan F, Lv LY, Liu J-M (2007) Thin Solid Films 515:5366
20. Lee Y-H, Lee C-C, Liu Z-X, Liang C-S, Wu J-M (2005) Electr Sol Stat Lett 9:38
21. Tian W, Vaithyanathan V, Schlom DG, Zhan Q, Yang SY, Chu YH, Ramesh R (2007) Appl Phys Lett 90:172908
22. Singh SK, Maruyama K, Ishiwara H (2007) J Phys D Appl Phys 40:2705
23. Yang SY, Zavaliche F, Mohaddes-Ardabili L, Vaithyanathan V, Schlom DG, Lee YJ, Chu YH, Cruz MP, Zhan Q, Zhao T, Ramesh R (2005) Appl Phys Lett 87:102903
24. Simões AZ, Gonzalez AHM, Cavalcante LS, Riccardi CS, Longo E, Varela JA (2007) J Appl Phys 101:074108
25. Cavalcante LS, Simões AZ, Santos LPS, Santos MRMC, Longo E, Varela JA (2006) J Solid State Chem 179:3739
26. Gao F, Cai C, Wang Y, Dong S, Qiu XY, Yuan GL, Liu ZG, Liu J-M (2006) J Appl Phys 99:094105
27. Das SR, Bhattacharya P, Choudhary RNP, Katiyara RS (2006) J Appl Phys 99:066107
28. Das SR, Choudhary RNP, Bhattacharya P, Katiyara RS, Dutta P, Manivannan A, Seehra MS (2007) J Appl Phys 101:034104
29. Pontes FM, Leite ER, Longo E, Varela JA, Araújo EB, Eiras JA (2000) Appl Phys Lett 76:2433
30. Chaneliere C, Autran JL, Devine RAB, Balland B (1996) Mater Sci Eng R 22:269
31. Pabst GW, Martin LW, Chu Y-H, Ramesh R (2007) Appl Phys Lett 90:072902
32. Simões AZ, Ramírez MA, Gonzalez AHM, Riccardi CS, Ries A, Longo E, Varela JA (2006) J Solid State Chem 179:2206